

# Journal Pre-proof

Modulating sustained drug release from nanocellulose hydrogel by adjusting the inner geometry of implantable capsules

Vili-Veli Auvinen, Juhani Virtanen, Arto Merivaara, Valtteri Virtanen, Patrick Laurén, Sampo Tuukkanen, Timo Laaksonen



PII: S1773-2247(19)31217-1

DOI: <https://doi.org/10.1016/j.jddst.2020.101625>

Reference: JDDST 101625

To appear in: *Journal of Drug Delivery Science and Technology*

Received Date: 20 August 2019

Revised Date: 12 February 2020

Accepted Date: 25 February 2020

Please cite this article as: V.-V. Auvinen, J. Virtanen, A. Merivaara, V. Virtanen, P. Laurén, S. Tuukkanen, T. Laaksonen, Modulating sustained drug release from nanocellulose hydrogel by adjusting the inner geometry of implantable capsules, *Journal of Drug Delivery Science and Technology* (2020), doi: <https://doi.org/10.1016/j.jddst.2020.101625>.

This is a PDF file of an article that has undergone enhancements after acceptance, such as the addition of a cover page and metadata, and formatting for readability, but it is not yet the definitive version of record. This version will undergo additional copyediting, typesetting and review before it is published in its final form, but we are providing this version to give early visibility of the article. Please note that, during the production process, errors may be discovered which could affect the content, and all legal disclaimers that apply to the journal pertain.

© 2020 Published by Elsevier B.V.

The authors contributed to the production of the article “” as written below:

<sup>1</sup>Faculty of Engineering and Natural Sciences, Tampere University, P.O. Box 541, 33014 Tampere, Finland

<sup>2</sup>Division of Pharmaceutical Biosciences, Faculty of Pharmacy, University of Helsinki, P.O. Box 56, FI-00014, Finland

<sup>3</sup>Faculty of Medicine and Health Technology, Tampere University, P.O. Box 692, 33101 Tampere, Finland

---

Vili-Veli Auvinen<sup>1,2\*</sup>

The main author who performed the majority of the drug release experiments and writing of the article and supplementary material. Contributed greatly in planning and revisions, and drew most of the figures.

Juhani Virtanen<sup>3</sup>

Contributed to the design of the capsules, produced the CAD designs and performed 3D printing. In addition, wrote the part of the article covering the 3D printing methodology.

Arto Merivaara<sup>2</sup>

Aided in performing the drug release measurements and revising the article.

Valteri Virtanen<sup>3</sup>

Drew the first CAD designs, operated the 3D printer and participated in the optimization of the capsules wall thickness (leakage optimization).

Patrick Laurén<sup>2</sup>

Contributed to the planning and revisions of the article.

Sampo Tuukkanen<sup>3</sup>

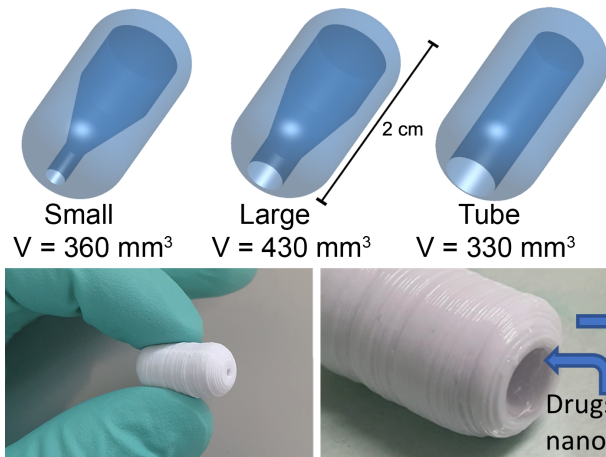
Contributed to the planning, supervising, and revisions of the article. He contributed to the initial ideas of the study.

Timo Laaksonen<sup>1</sup>

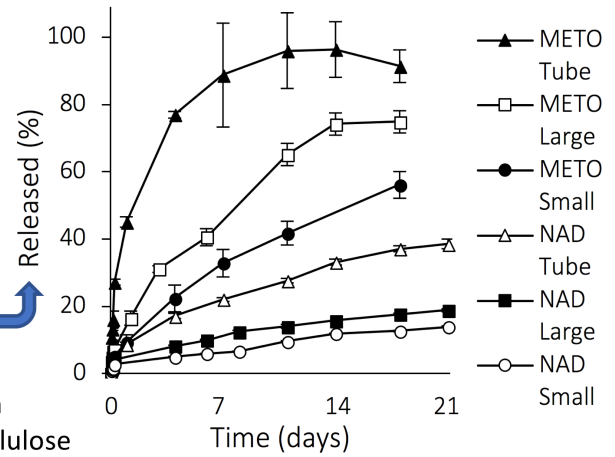
The main supervisor of the project. He wrote the result part for the Higuchi model and drew figure 4.

He contributed greatly to the planning and revising phases of the article.

3D printed PLA capsules filled with nanocellulose



*In vitro* release of metoprolol and nadolol



Journal Pre-proof

1  
2  
3 **Modulating sustained drug release from**  
4 **nanocellulose hydrogel by adjusting the inner**  
5 **geometry of implantable capsules**

6  
7  
8 Vili-Veli Auvinen<sup>1,2\*</sup>, Juhani Virtanen<sup>3</sup>, Arto Merivaara<sup>2</sup>, Valtteri Virtanen<sup>3</sup>, Patrick Laurén<sup>2</sup>, Sampo  
9 Tuukkanen<sup>3</sup>, Timo Laaksonen<sup>1</sup>

10  
11 <sup>1</sup>Faculty of Engineering and Natural Sciences, Tampere University, P.O. Box 541, 33014 Tampere, Finland

12 <sup>2</sup>Division of Pharmaceutical Biosciences, Faculty of Pharmacy, University of Helsinki, P.O. Box 56, FI-00014,  
13 Finland

14 <sup>3</sup>Faculty of Medicine and Health Technology, Tampere University, P.O. Box 692, 33101 Tampere, Finland

15  
16  
17 \*Corresponding author

18 Email: [yili.auvinen@tuni.fi](mailto:yili.auvinen@tuni.fi)

19 Tel. +358 294159131

20 Tampere University, P.O. Box 541, 33014 Tampere, Finland

21

## 22 **Abstract**

23 Nanocellulose hydrogel has been shown to be an excellent platform for drug delivery and it has  
24 been lately studied as an injectable drug carrier. 3D printing is an effective method for fast  
25 prototyping of pharmaceutical devices with unique shape and cavities enabling new types of  
26 controlled release. In this study, we combined the versatility of 3D printing capsules with  
27 controlled geometry and the drug release properties of nanocellulose hydrogel to accurately  
28 modulate its drug release properties. We first manufactured non-active capsules via 3D printing  
29 from biocompatible poly(lactic acid) (PLA) that limit the direction of drug diffusion. As a novel  
30 method, the capsules were filled with a drug dispersion composed of model compounds and  
31 anionic cellulose nanofiber (CNF) hydrogel. The main benefit of this device is that the release of  
32 any CNF-compatible drug can be modulated simply by modulating the inner geometry of the  
33 PLA capsule. In the study we optimized the size and shape of the capsules inner cavity and  
34 performed drug release tests with common beta blockers metoprolol and nadolol as the model  
35 compounds. The results demonstrate that the sustained release profiles provided by the CNF  
36 matrix can be accurately modulated via adjusting the geometry of the 3D printed PLA capsule,  
37 resulting in adjustable sustained release for the model compounds.

38

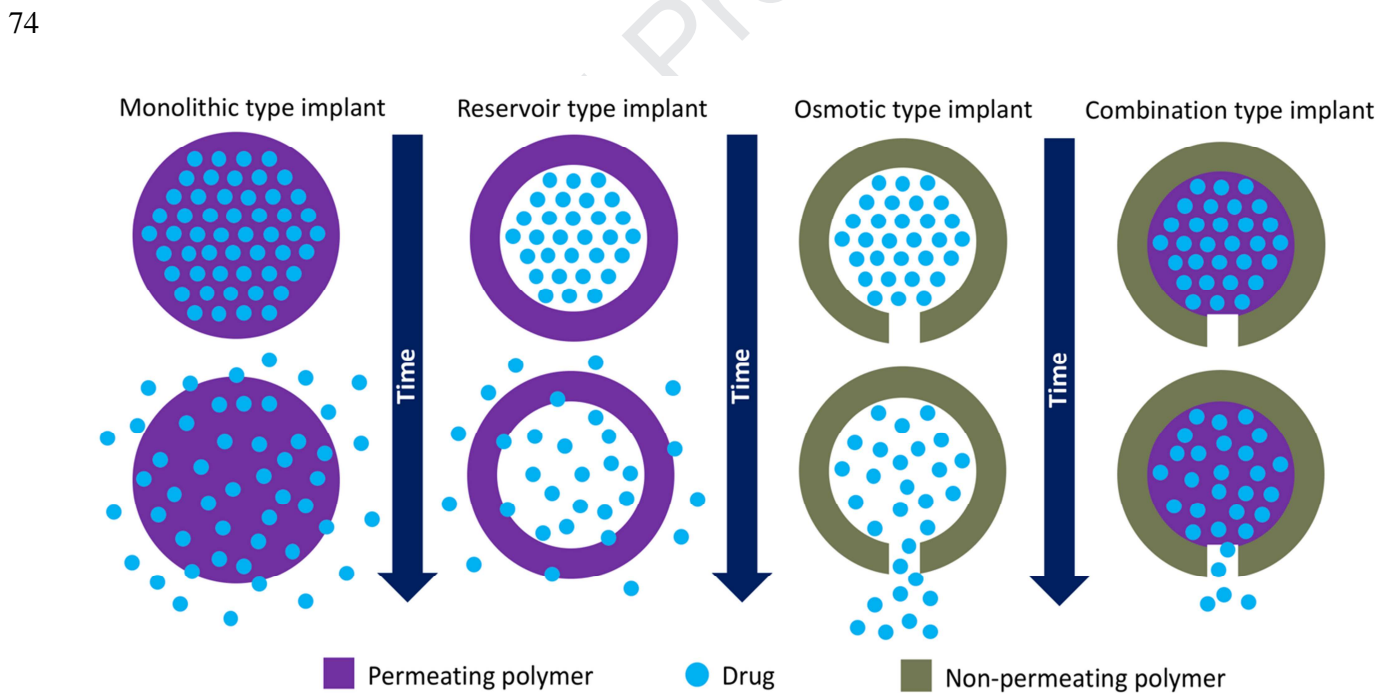
39 **Keywords:** 3D printing, nanocellulose, hydrogel, sustained drug release

## 40 **1 Introduction**

41  
42 The increased access to 3D printers has accelerated the development of new products and  
43 applications for drug release device development on the pharmaceutical field. These  
44 breakthroughs include 3D printing bilayers of different medicinal compounds into single oral  
45 dosage forms, oral tablets with inner channels and porous structures and adjustments on the  
46 geometry of printed oral capsules allowing customization of the drug release [1-5]. However, the  
47 usage of such geometrical innovations has not yet boomed on the rapidly growing market of  
48 implantable polymeric drug release devices [6]. These devices can be classified into four groups:  
49 passive polymeric implants, non-biodegradable polymeric implantable systems, biodegradable  
50 implants and dynamic or active implants [6]. In addition, the drug release mechanisms from such  
51 devices can be classified into four categories: controlled swelling, matrix degeneration, passive  
52 diffusion and osmotic pumping [7]. For implementation of drug release devices there are  
53 typically three main sites: subcutaneous, intra-vaginal and intra-vesical. [6] The usage of  
54 subcutaneous drug releasing devices is an invasive process and typically leaves permanent  
55 scarring. However, this can be the preferred treatment option when compared to continuous  
56 injections or daily pills or the drug implant has other benefits compared to oral dosing such as in  
57 the complex case of opioid addicted patients [8, 9].

58  
59 Controlled swelling, passive diffusion and matrix degeneration have a key role in monolithic and  
60 reservoir type implants [6], which have been illustrated in Figure 1. In osmotic type implants, a  
61 non-permeating polymer is used and the osmotic gradient creates a stable inflow of body fluid  
62 within the device [10]. This increases the pressure inside the implant and forces drug release  
63 through the opening as shown in Figure 1 [10]. Such design produces a constant drug release with

64 zero order kinetics [10]. Some monolithic implants feature no solid structures but instead rely on  
 65 injectable drug releasing hydrogel formulations. Two recent interesting applications are a  
 66 nanogel-based *in situ* forming implant for HIV drug release [11] and an application where CNF  
 67 hydrogel formulations were subcutaneously injected in mice [12]. The injected CNF hydrogels  
 68 operated as a monolithic type implant; the hydrogel had a high drug loading and the implant did  
 69 not migrate or degrade despite the free movement of the mice [12]. In our work, we studied the  
 70 use of a CNF hydrogel formulation as monolithic drug dispersions but inside a combination type  
 71 implant illustrated in Figure 1. Successful clinical testing has been performed with a similar  
 72 device, comprising of a simple cylindrical capsule filled with a 2-hydroxyethyl methacrylate  
 73 hydrogel and a therapeutic agent [13].



75

76 **Fig 1. An illustration of monolithic, reservoir, osmotic and combination type implants.**

77



78 Cellulose-based nanostructured materials, generally known as a family of nanocelluloses, are  
79 interesting biocompatible materials, which have shown benefits in numerous medical  
80 applications [14]. Nanocellulose can be produced in three types: as bacterial cellulose (BC),  
81 cellulose nanocrystals (CNC) and as cellulose nanofibers (CNF) [15]. The cellulose nanofibers  
82 can be chemically modified by TEMPO [(2,2,6,6-tetramethylpiperidin-1-yl)oxyl] oxidation to  
83 manufacture anionic cellulose nanofibers [16, 19]. Lately, especially anionic CNF hydrogels  
84 have been shown to operate as a semi-universal drug matrix for the release of different types of  
85 molecules (small, large, cationic and anionic) [18, 19]. In addition, CNF has been used to  
86 manufacture drug-loaded film-like matrix systems with long-lasting sustained release for up to  
87 three months [20].

88  
89 Conventional 3D printing typically involves heat or other manufacturing methods that limit its  
90 suitability for biomolecules, such as proteins and lipids [21]. The 3D printed drug delivery  
91 systems might further have an uneven or porous surface affecting the rate of the drug release,  
92 especially in extrusion and powder printing [22]. Extrusion, powder and inkjet-based printing  
93 require post-operative drying, which is an additional process variable affecting the appearance  
94 and the properties of the product [23]. However, it is possible to overcome these limitations by  
95 first printing customized capsules from an inert biocompatible material and then fill the capsules  
96 with sensitive drugs or biomolecules together with a release rate-controlling matrix material [24].  
97 It is also possible to subsequently print a drug dosing cap to further enhance and modulate the  
98 sustained release profile [21, 24].

99

100 In this study, we combine the new possibilities of printing specifically designed drug capsules  
101 and the recent advances in the implantation of CNF hydrogels into three rapid prototyped designs  
102 and evaluate their properties *in vitro* as sustained release devices. Traditionally in pharmaceutical  
103 hydrogel applications, the release rate of the drug is controlled by the concentration of the loaded  
104 drug and other active ingredients [25]. Here, a similar effect is expected by controlling the inner  
105 geometry of the capsule which limits drug diffusion from the hydrogel. The idea differs from the  
106 previously mentioned drug release devices and hydrogels as the release is fundamentally  
107 controlled by the inner hydrogel, which facilitates a sustained release profile while the release  
108 can be further modulated via the geometry of the inner cavity of the capsule.

109

## 110 **2 Materials and Methods**

### 111 112 **2.1 Materials**

113 2.7% (lot 11724) anionic CNF hydrogel Fibdex<sup>TM</sup> was purchased from UPM-Kymmene Oyj,  
114 Finland. PrimaValue<sup>TM</sup> poly(lactic acid) (PLA) filaments were purchased from 3D Prima,  
115 Malmö, Sweden. Nadolol, metoprolol tartrate and methylene blue, were purchased from Sigma-  
116 Aldrich, USA. Dulbecco's Phosphate Buffered Saline (10×) concentrate without calcium and  
117 magnesium was purchased from Gibco, UK. The buffer solution used was made in double  
118 distilled ultrapure water.

### 119 **2.2 Printing of PLA capsules**

120 The capsules were modeled with Onshape (Onshape inc, Cambridge, USA) Computer Aided  
121 Design (CAD) software and the CAD model was later processed with Slic3r -software package  
122 to produce the actual printing data. Capsules were printed from commercially available PLA  
123 filaments using fused deposition modeling (FDM) printing process. The FDM process is  
124 essentially an extrusion method where a heated material, in this case PLA, is directed through a  
125 nozzle and deposited in x, y and z space to to produce 3D constructs on the printing stage. In this  
126 study, the capsules were printed with 100% infill to ensure the sufficient barrier properties of the  
127 printed walls. 3D printing was carried out using PRUSA I3 MK2 (Prusa research, s.r.a., Praha,  
128 Czech republic) at 210 °C with a printing rate of 40 mm/s and 0.2 mm layer height. The printer  
129 nozzle diameter during the printing was 0.4 mm. No post processing, such as smoothing after the  
130 printing, was performed, however each capsule used in the experiments was hand-picked so that  
131 no visible unevenness around the release channel could be observed. The length of each  
132 produced capsule was 20 mm, and the width 10 mm. The diameter of the bottleneck was 2.0 mm

133 for small, 3.6 mm for large and 5.0 mm for tube design leading into shared constant flat surface  
134 areas of 3.1 mm<sup>2</sup> for small, 10 mm<sup>2</sup> for large and 19 mm<sup>2</sup> for the tube design. The inner total  
135 volumes were 360 mm<sup>3</sup> for the small, 430 mm<sup>3</sup> for the large and 330 mm<sup>3</sup> for the tube design.

136

### 137 **2.3 Leakage tests and injection of hydrogel formulations**

138 After the manufacturing of the capsules, leakage tests were performed using methylene blue as a  
139 dye for visual observation of possible leaks. First, a dyed hydrogel was made by mixing anionic  
140 CNF hydrogel with methylene blue and injecting it inside the capsules with standard 19G  
141 needles. The capsules were weighted before and after injection to ensure that a complete filling  
142 had been accomplished and to rule out the presence of air bubbles. Next, the capsules were wet  
143 and any leakage of the blue color through the core was observed with a slow-motion camera.

144

### 145 **2.4. Preparation of the hydrogel formulations**

146 The hydrogel formulations were prepared by mixing anionic CNF hydrogel with the model  
147 compounds. The mixing was performed by connecting two 10 ml syringes from their nozzles  
148 with a tiny rubber hose and then pushing the contents of each syringe to the other via the hose.  
149 The anionic CNF hydrogel (fiber content 2.7%) was weighted directly in the syringes and  
150 nadolol or metoprolol was added as a dry powder. Nadolol and metoprolol were loaded in excess  
151 amount to form monolithic dispersions. The formulations were then homogenized by pushing the  
152 contents back and forth through the hose for 5 min. The final amount of cellulose nanofibers in  
153 both formulations was 1.8 %. The total amount of metoprolol inside the capsules was 152 mg for  
154 the large design, 130 mg for the small design and 105 mg for the tube design. For nadolol, the  
155 amounts were 131 mg for the large capsule, 110 mg for the small design and 91 mg for the tube

156 design. The used quantity for nadolol represents concentration of 0.89 M. The solubility of  
157 nadolol in water is 0.03 M, meaning that the water-based hydrogel formulation can be  
158 characterized as a monolithic dispersion [26]. The solubility for metoprolol tartrate in water is  
159 much higher and therefore its solubility in the 2.7% ANFC hydrogel was tested separately with  
160 nephelometry. The results show that the hydrogel does not possess enough free water to dilute all  
161 of the added metoprolol, resulting in a monolithic dispersion. The measured solubility data for  
162 metoprolol is shown in the supplementary data.

163

## 164 **2.5 In vitro drug release studies**

165 The 3D printed capsules were filled with formulated hydrogels via injection with standard 19G  
166 needles and the visible hydrogel surface was evened with plastic strips. The capsules were  
167 weighted before and after injection to ensure that a complete filling had been accomplished and  
168 to rule out the presence of air bubbles. The filled capsules were placed in glass bottles with 70 ml  
169 of phosphate buffered saline (1 x DPBS) and kept at 37 °C incubator shaker (Innova 4400, by  
170 ALLERGAN. Inc.) under constant shaking at 150 RPM for 3 weeks, except the small and large  
171 designs for nadolol were measured for 5 weeks. At chosen time points, 1 ml was collected from  
172 each sample and replaced with 1 ml of fresh buffer. The amount of removed model compound  
173 from each time point was mathematically added to the next time point in order to plot cumulative  
174 release. All experiments were performed in triplicate.

175

## 176 **2.6 Quantification of released model compounds**

177 The concentrations of nadolol and metoprolol from the *in vitro* release tests were analyzed with  
178 Ultra performance liquid chromatography (UPLC) instrument Acquity UPLC (Waters, USA).

179 For nadolol and metoprolol, the used column was HSS-T3 1.8  $\mu\text{m}$  (2.1  $\times$  50 mm) (Waters, USA)  
180 at 30 °C. The injection volume for nadolol was 5  $\mu\text{l}$  and 2  $\mu\text{l}$  for metoprolol and the flow rate was  
181 0.5 ml/min for both compounds. The detection of nadolol and metoprolol was performed at the  
182 wavelengths of 215 nm and 221 nm, respectively. During the gradient run the mobile phase  
183 consisted of a mixture of acetonitrile and 15 mM phosphate buffer at pH 2 in 10:90 ratio for  
184 nadolol and 20:80 for metoprolol. The retention times were 0.92 min for nadolol and 0.89 min  
185 for metoprolol.

186

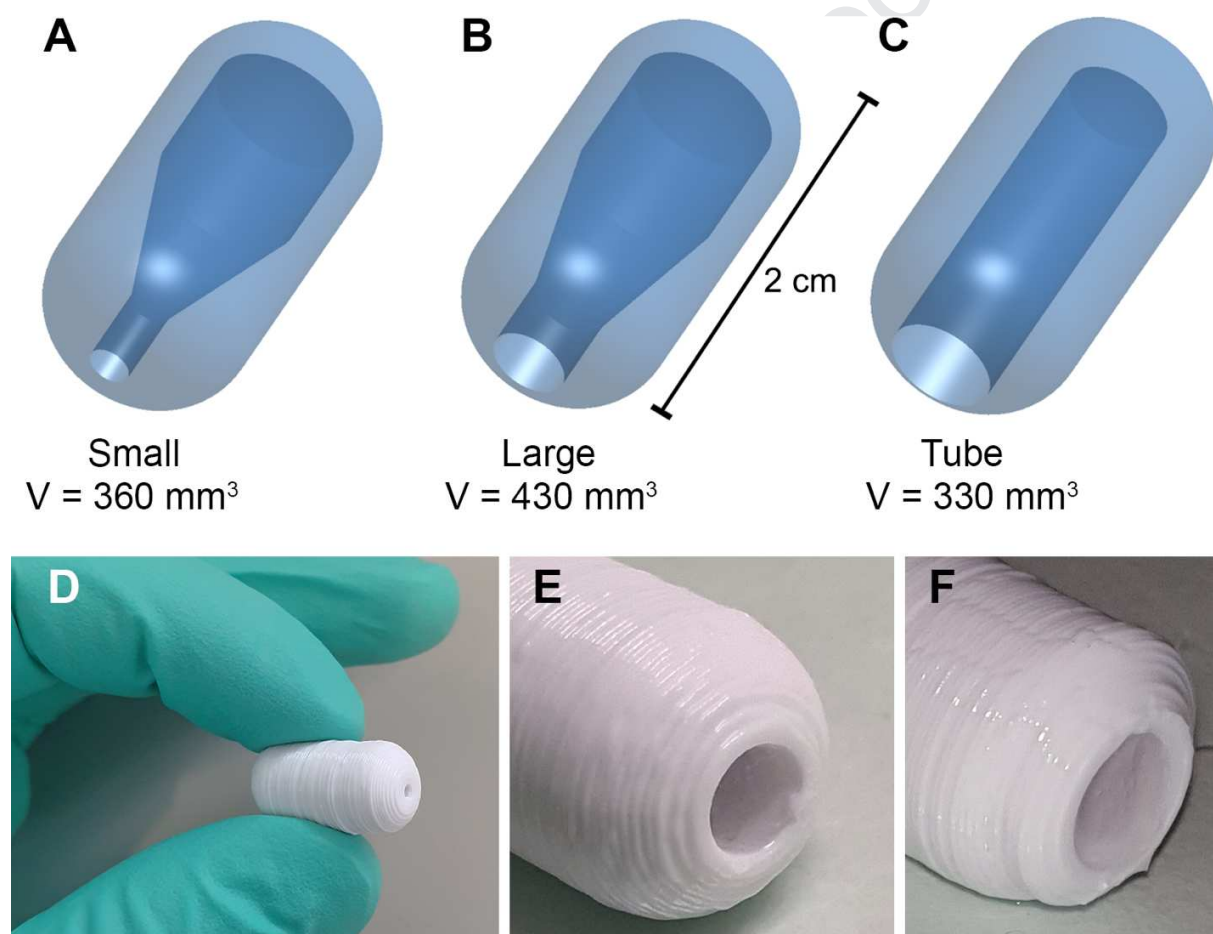
### 187 **3 Results and Discussion**

188 We designed capsules that had an inner reservoir cavity for the CNF hydrogel and a single  
189 release channel (to which we will be later referring as bottleneck). Outer measurements for each  
190 design were 10 mm x 20 mm and the capsules were 3D printed from PLA using fused deposition  
191 modelling (FDM) and filled with a suspension made of anionic CNF hydrogel and the model  
192 compounds, nadolol and metoprolol, which are both commonly used beta blockers. Nadolol's  
193 release profile from anionic CNF hydrogels have been characterized previously, where 90% of  
194 the loaded nadolol diffused out of the hydrogel during one week [18]. PLA and anionic CNF  
195 hydrogel were chosen as materials for the capsules, as both are biocompatible materials (in  
196 humans) and biodegradable (in nature) [27-30].

197

198 The designs of the manufactured capsules are visualized in Figure 2 (A-C) and with exact  
199 measurements in the supplementary material. The bottlenecks lead into inner cavities, which  
200 were filled with the anionic CNF hydrogel containing the studied model compound. We will  
201 refer to the different structures as small (Fig 2A), large (Fig 2B), and tube (Fig 2C) designs. The

202 designs presented here allow for a wide range of customization. As the PLA capsule carries and  
203 regulates the open surface area of the anionic CNF hydrogel, which operates as a matrix for the  
204 model compounds, the drug release can be controlled by modifying the characteristics of either  
205 component. However, as the release properties of anionic CNF hydrogels have been established  
206 previously [18], we focused on the geometry of the PLA capsule and demonstrate that flexible  
207 control over the release rate can be achieved with minimal changes to the inner matrix.  
208



209  
210 **Fig 2. Computer aided designs (A-C) and 3D printed versions (D-F) of the studied PLA**  
211 **capsules.** (A) Small capsule. (B) Large capsule. (C) Tube design. (D) A 3D printed PLA capsule  
212 (small). (E-F) The large and tube designs filled with a hydrogel formulation after 3 weeks in

213 DPBS buffer still showing an even surface of the hydrogel. The image (F) has been taken with  
214 camera flash on to highlight the normally transparent anionic CNF hydrogel.

215

### 216 **3.1 Leakage tests and optimization of the PLA capsules**

217 The designs were first optimized not to leak via prototyping. Figure 2 shows the final optimized  
218 designs. We particularly had to optimize the bottom thickness as our first designs with a thin  
219 bottom leaked from the edges of the inner cavities. The combination of 3D printing and separate  
220 injection of the hydrogel allowed bypassing any requirements set by the FDM printing such as  
221 the required flow properties of the drugs [31]. The model compounds metoprolol and nadolol did  
222 not undergo any temperatures above 37 °C during the study, suggesting that the method would  
223 be compatible with biomolecules such as lipids and proteins. The final optimized designs are  
224 presented in Figure 2 A-C and with exact measurements in the supplementary data (Fig S1).

225

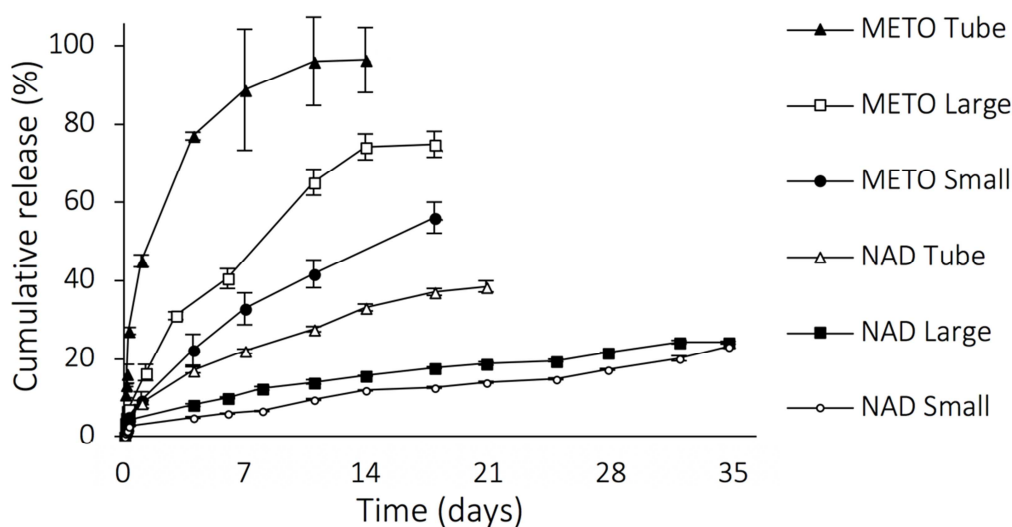
### 226 **3.2 Sustained in vitro release of the model compounds**

227 During the three-week release study, a sustained release profile was obtained for both model  
228 compounds with all three PLA capsule designs. As expected, the small design with the smallest  
229 surface area in contact with the external buffer sustained the release the most for both model  
230 compounds. The large design had less effect on sustaining the release, and the tube design  
231 sustained the release the least. The results are shown in Figure 3, where the top three lines  
232 represent the release of the metoprolol filled PLA capsules, and the bottom three the nadolol  
233 filled PLA capsules. During the first hours all capsules released the model compounds rapidly  
234 and after the initial drug release the release rate was observed as linear. For the tube design with  
235 metoprolol, the highest total release of 96.4% was reached on the 14<sup>th</sup> day. No swelling nor



236 collapsing of the hydrogels were visually observed during the three-week measurements, as  
 237 shown in Figure 2 E still showing an even surface of hydrogel, matching the results of  
 238 Paukkonen et al. [18]. After 14 days, the amount of metoprolol in the buffer appeared to decrease  
 239 (data not shown). This is due to the hydrolysis of nadolol and metoprolol in aqueous conditions  
 240 [32]. However, in the case of nadolol, this was not observable due to extremely sustained release,  
 241 which allows a part of the drug dose to remain in crystallized form inside the hydrogel and hence  
 242 delay the hydrolysis. As the hydrogels contained a significant amount of undissolved drug  
 243 maintaining a constant reservoir system, the hydrogels can be characterized as monolithic  
 244 dispersions. We performed solubility measurement for metoprolol in anionic CNF hydrogel with  
 245 nephelometry and the results are shown in the supplementary data (Fig S2).

246



247

248 **Fig 3.** Scaled cumulative release of the model compounds metoprolol (METO) and nadolol  
 249 (NAD) from the three capsule designs (Tube, Large, and Small) carrying anionic cellulose  
 250 nanofiber hydrogel drug formulations (mean  $\pm$  S.D., n = 3). The experiments were conducted at  
 251 37 °C in DPBS buffer.

252

253 **3.2 Mathematical model for the release**

254 For monolithic dispersions with flat release areas, the release rate is expected to follow the  
 255 Higuchi equation (1) [33].

256

$$257 \quad f = \frac{A}{M_{\text{loaded}}} \sqrt{Dc_s(2c_{\text{ini}} - c_s) \times t} = \frac{A}{V} \sqrt{Dc_s/c_{\text{ini}}^2(2c_{\text{ini}} - c_s) \times t} \quad (1)$$

258

259 where  $f$  is the fraction of the drug released,  $M_{\text{loaded}}$  is amount of the drug initially loaded into  
 260 the capsule,  $A$  is the surface area exposed to the release buffer,  $D$  is the diffusion coefficient of  
 261 the drug,  $c_s$  is the solubility of the drug,  $c_{\text{ini}}$  is the concentration of the drug initially inside the  
 262 inner cavity (0.991 mol/L for nadolol and 1.15 mol/L for metoprolol),  $V$  is the total volume of  
 263 the hydrogel formulation, and  $t$  is time. The solubilities in water (at 25 °C), for nadolol and  
 264 metoprolol are 8330 and 402 mg/L (at 25 °C), respectively.

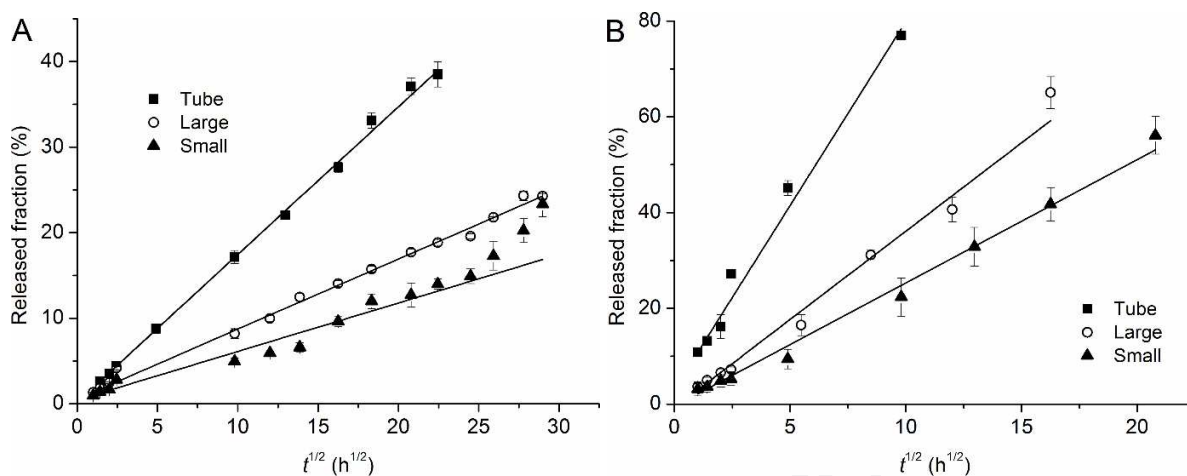
265

266 When the released fractions are then plotted against  $\sqrt{t}$ , the curves should be linear and the  
 267 slopes ( $k$ ) should be dependent on the area exposed to the release buffer divided by the total  
 268 volume of the hydrogel. These plots are shown in Figure 4. The Eq. (1) can be further simplified  
 269 to Eq. (2) by combining drug-dependent parameters variables to a constant  $K$  ( $K =$   
 270  $(Dc_s/c_{\text{ini}}^2(2c_{\text{ini}} - c_s))^{1/2}$ ) and drug-independent design parameters to a constant  $a$  ( $a = A/V$ ),  
 271 which is related to the geometry of the capsules.

272

$$273 \quad f = aK\sqrt{t} = k\sqrt{t} \quad (2)$$

274



275  
276 **Fig 4.** Fitted Higuchi equations (lines) to the nadolol (A) and metoprolol (B) release data for all  
277 three capsule designs (Tube, Large, and Small). The data points are the same as in Figure 3 but  
278 only the part of the data with no evident drug degradation was used for the fitting.

279  
280 The slopes from Figure 4, and the corresponding values of the formulation parameters  $a$  are  
281 shown in Table 1. For metoprolol, only the parts of the release curves where no clear degradation  
282 of the drug was seen were used to do the theoretical fits. It is worth noting that in an ideal case,  
283 the release rate would be completely controlled by the design parameter  $a$ , as  $K$  was constant for  
284 each drug release series, however, a number of things such as swelling or more complex  
285 geometries can lead to deviations from the standard Higuchi equation. Any visible swelling  
286 could be ruled out based on visual observations of the capsules in buffer solutions before and  
287 after the measurements. However, an analysis of the ratios of the slopes to the ratios of  $a$  will  
288 indicate how well the release curves fit the Higuchi equation and helps in verifying the release  
289 mechanism, since in our case we should have  $a_1/a_2 = k_1/k_2$  for any two different designs.

290

291 **Table 1.** Slopes from the release rate fitting in Figure 4 and a comparison of the design variables  
 292 ( $a$ ) indicating ideal release behavior to the slopes ( $k$ ) of the real release rates. The parameters are  
 293 normalized to those obtained for the tube-design.

	Design parameter ratios	$k$		$k/k_{\text{tube}}$		$R^2$	
		Metoprolol	Nadolol	Metoprolol	Nadolol	Metoprolol	Nadolol
Tube	$a/a_{\text{tube}}$ 1.00	7.69	1.73	1.00	1.00	0.99	1.00
Large	$a/a_{\text{tube}}$ 0.37	3.69	0.82	0.48	0.47	0.99	1.00
Small	$a/a_{\text{tube}}$ 0.13	2.58	0.57	0.34	0.33	0.99	0.91

294  
 295  
 296 All the designs could be modeled with the Higuchi equation. Especially the release data from the  
 297 tube-design shows excellent near-perfect fits to Eq. (1). The equation is theoretically derived for  
 298 a case very much like our current design [34]. And although the release rate from the large  
 299 bottleneck was slightly faster than expected, the ratio of the design parameters and the ratios of  
 300 the slopes of the large and tube designs are close to each other (0.374 vs. 0.480 and 0.474),  
 301 indicating similar release mechanism as in the case of the tube design. In the case of the small  
 302 bottleneck, a larger deviation from theory was seen and the release rate was much faster than  
 303 would have been expected (0.132 vs. 0.335). The reason is that the Higuchi equation only  
 304 describes release from the neck of the capsule, i.e. from a system with constant cross-section to  
 305 volume ratio. As the bottleneck is quite short, it is not able to control the release rate alone. At  
 306 some point during the release experiment, the diffusion from the larger inner cavity to the neck  
 307 part will start to dominate the release kinetics. In this area, the cross section to volume ratio of  
 308 the large and small designs are similar. And that is why we see that the slopes of these two  
 309 designs start approaching each other later in the release measurements. The jump to higher

310 release fractions for the large design in the early stage of the release is due to the difference in  
311 the cross-section to volume ratios inside the neck of the capsule.

312

313 As the release rates for several types of molecules has been measured for the same CNF hydrogel  
314 grade [18], we can estimate the release rates of various therapeutical molecules for our implant.

315 In addition, the same CNF hydrogel grade has been proven to be freeze-dryable without the loss  
316 of rheological properties nor any changes in its release profile [18]. For subcutaneous

317 implantation the thickness of the capsule walls could be decreased for increased comfort and  
318 patient compliance. Despite PLA being an excellent material for the current *in vitro* tests, the

319 material could be further enhanced to prevent foreign body reaction and bacterial growth. Recent  
320 breakthroughs include foreign body resistant materials [35]. To prevent biofilm formation in *in*

321 *vivo* environment, antimicrobial material such as nitrofurantoin can be mixed with the PLA [36-  
322 37]. In addition, the outer surface of the PLA capsule can be post-operated smoother to reduce

323 surface area for biofilm formation [36].

324

## 325 **4 Conclusions**

326

327 In summary, the obtained leakage tests and *in vitro* results from model compounds demonstrate  
328 the suitability of the CNF hydrogel filled 3D printed PLA capsules as sustained release platforms

329 without the use of any additional excipients. The diameter of the capsules release channel  
330 (“bottleneck”) can be modified effortlessly resulting in several adjustable parameters together

331 with the drug and hydrogel concentrations and a high control over the release rate. From the  
332 theoretical analysis of the results it can be concluded that the tube and the large designs can be

333 modeled by the Higuchi equation. As the neck is made thinner, internal diffusion kinetics  
334 become more complicated and deviations from theory are seen. Nevertheless, a control over the  
335 release rates was maintained and the behavior of all systems can be explained by the varying  
336 cross-section to volume ratios. As the capsules are injected with the hydrogel formulations post-  
337 printing, the drug substances do not undergo heating, resulting in wide compatibility for  
338 therapeutic compounds such as proteins and liposomes. In the future, the actual injection of the  
339 hydrogel formulations could be performed automatically by 3D printers and an antimicrobial  
340 PLA feedstock could be implemented in the FDM printing.

341

## 342 **5 Acknowledgements**

343

344 The authors acknowledge and thank the University of Helsinki for co-operation and for  
345 providing access to their laboratories and screening instrumentation.

346

## 347 **6 References**

348

349 [1] Khaled, S. A., Burley, J. C., Alexander, M. R., & Roberts, C. J. (2014). Desktop 3D printing  
350 of controlled release pharmaceutical bilayer tablets. *International journal of pharmaceutics*,  
351 *461*(1-2), 105-111.

352

353 [2] Sadia, M., Arafat, B., Ahmed, W., Forbes, R. T., & Alhnan, M. A. (2018). Channeled tablets:  
354 An innovative approach to accelerating drug release from 3D printed tablets. *Journal of*  
355 *Controlled Release*, *269*, 355-363.

- 356
- 357 [3] Goyanes, A., Martinez, P. R., Buanz, A., Basit, A. W., & Gaisford, S. (2015). Effect of  
358 geometry on drug release from 3D printed tablets. *International journal of pharmaceutics*,  
359 *494*(2), 657-663.
- 360
- 361 [4] Khaled, S. A., Burley, J. C., Alexander, M. R., Yang, J., & Roberts, C. J. (2015). 3D printing  
362 of five-in-one dose combination polypill with defined immediate and sustained release profiles.  
363 *Journal of Controlled Release*, *217*, 308-314.
- 364
- 365 [5] Skorywa et al., Fabrication of extended-release patient-tailored prednisolone tablets via fused  
366 deposition modelling (FDM) 3D printing
- 367
- 368 [6] Stewart, S. A., Domínguez-Robles, J., Donnelly, R. F., & Larrañeta, E. (2018). Implantable  
369 polymeric drug delivery devices: Classification, manufacture, materials, and clinical  
370 applications. *Polymers*, *10*(12), 1379.
- 371
- 372 [7] Kleiner, L. W., Wright, J. C., & Wang, Y. (2014). Evolution of implantable and insertable  
373 drug delivery systems. *Journal of controlled release*, *181*, 1-10.
- 374
- 375 [8] Itzoe, M., & Guarnieri, M. (2017). New developments in managing opioid addiction: impact  
376 of a subdermal buprenorphine implant. *Drug design, development and therapy*, *11*, 1429.
- 377

- 378 [9] Ling, W., Casadonte, P., Bigelow, G., Kampman, K. M., Patkar, A., Bailey, G. L., ... &  
379 Beebe, K. L. (2010). Buprenorphine implants for treatment of opioid dependence: a randomized  
380 controlled trial. *Jama*, 304(14), 1576-1583.
- 381
- 382 [10] Kumar, A., & Pillai, J. (2018). Implantable drug delivery systems: An overview. In  
383 Nanostructures for the Engineering of Cells, Tissues and Organs (pp. 473-511). William Andrew  
384 Publishing. KUMAR, Anoop; PILLAI, Jonathan. Implantable drug delivery  
385
- 386 [11] Town, A. R., Taylor, J., Dawson, K., Niezabitowska, E., Elbaz, N. M., Corker, A., ... &  
387 McDonald, T. O. (2019). Tuning HIV drug release from a nanogel-based in situ forming implant  
388 by changing nanogel size. *Journal of Materials Chemistry B*, 7(3), 373-383.
- 389
- 390 [12] Laurén, P., Lou, Y., Raki, M., Urtti, A., Bergström, K., Yliperttula, M., 2014. Technetium-  
391 99m-labeled nanofibrillar cellulose hydrogel for in vivo drug release. *Eur. J. Pharm. Sci.* 65, 79–  
392 88.
- 393
- 394 [13] Kuzma, P., Moo-Young, A. J., Mora, D., Quandt, H., Bardin, C. W., & Schlegel, P. H.  
395 (1996, May). Subcutaneous hydrogel reservoir system for controlled drug delivery. In  
396 *Macromolecular Symposia* (Vol. 109, No. 1, pp. 15-26). Basel: Hüthig & Wepf Verlag.
- 397
- 398 [14] Moon, R. J., Martini, A., Nairn, J., Simonsen, J., & Youngblood, J. (2011). Cellulose  
399 nanomaterials review: structure, properties and nanocomposites. *Chemical Society*  
400 *Reviews*, 40(7), 3941-3994.



- 401
- 402 [15] Plackett, D., Letchford, K., Jackson, J., & Burt, H. (2014). A review of nanocellulose as a  
403 novel vehicle for drug delivery. *Nordic Pulp & Paper Research Journal*, 29(1), 105-118.
- 404
- 405 [16] Saito, T., Nishiyama, Y., Putaux, J. L., Vignon, M., & Isogai, A. (2006). Homogeneous  
406 suspensions of individualized microfibrils from TEMPO-catalyzed oxidation of native cellulose.  
407 *Biomacromolecules*, 7(6), 1687-1691.
- 408
- 409 [17] Saito, T., Kimura, S., Nishiyama, Y., & Isogai, A. (2007). Cellulose nanofibers prepared by  
410 TEMPO-mediated oxidation of native cellulose. *Biomacromolecules*, 8(8), 2485-2491.
- 411
- 412 [18] Paukkonen, H., Kunnari, M., Laurén, P., Hakkarainen, T., Auvinen, V. V., Oksanen, T., ...  
413 & Laaksonen, T. (2017). Nanofibrillar cellulose hydrogels and reconstructed hydrogels as  
414 matrices for controlled drug release. *International journal of pharmaceutics*, 532(1), 269-280.
- 415
- 416 [19] Gupta, P., Vermani, K., & Garg, S. (2002). Hydrogels: from controlled release to pH-  
417 responsive drug delivery. *Drug discovery today*, 7(10), 569-579.
- 418
- 419 [20] Kolakovic, R., Peltonen, L., Laukkanen, A., Hirvonen, J., & Laaksonen, T. (2012).  
420 Nanofibrillar cellulose films for controlled drug delivery. *European Journal of Pharmaceutics  
421 and Biopharmaceutics*, 82(2), 308-315.
- 422

- 423 [21] Alhnan, M. A., Okwuosa, T. C., Sadia, M., Wan, K. W., Ahmed, W., & Arafat, B. (2016).  
424 Emergence of 3D printed dosage forms: opportunities and challenges. *Pharmaceutical research*,  
425 33(8), 1817-1832.  
426
- 427 [22] Pham, D. T., & Gault, R. S. (1998). A comparison of rapid prototyping technologies.  
428 *International Journal of machine tools and manufacture*, 38(10-11), 1257-1287.  
429
- 430 [23] Gaylo, C. M., Pryor, T. J., Fairweather, J. A., & Weitzel, D. E. (2006). *U.S. Patent No.*  
431 *7,027,887*. Washington, DC: U.S. Patent and Trademark Office.  
432
- 433 [24] Genina et. al. Anti-tuberculosis drug combination for controlled oral delivery using 3D  
434 printed compartmental dosage forms: From drug product design to in vivo testing. *J Control*  
435 *Release*. 2017 Dec 28; 268:40-48. doi: 10.1016/j.jconrel.2017.10.003.  
436
- 437 [25] Slaughter, B. V., Khurshid, S. S., Fisher, O. Z., Khademhosseini, A., & Peppas, N. A.  
438 (2009). Hydrogels in regenerative medicine. *Advanced materials*, 21(32-33), 3307-3329.  
439
- 440 [26] McFarland, J. W., Avdeef, A., Berger, C. M., & Raevsky, O. A. (2001). Estimating the  
441 water solubilities of crystalline compounds from their chemical structures alone. *Journal of*  
442 *chemical information and computer sciences*, 41(5), 1355-1359.  
443

- 444 [27] Chinga-Carrasco, G., & Syverud, K. (2014). Pretreatment-dependent surface chemistry of  
445 wood nanocellulose for pH-sensitive hydrogels. *Journal of biomaterials applications*, 29(3),  
446 423-432.
- 447
- 448 [28] Lin, N., & Dufresne, A. (2014). Nanocellulose in biomedicine: Current status and future  
449 prospect. *European Polymer Journal*, 59, 302-325.
- 450
- 451 [29] Powell, L. C., Khan, S., Chinga-Carrasco, G., Wright, C. J., Hill, K. E., & Thomas, D. W.  
452 (2016). An investigation of *Pseudomonas aeruginosa* biofilm growth on novel nanocellulose  
453 fibre dressings. *Carbohydrate polymers*, 137, 191-197.
- 454
- 455 [30] Zhang, Y., Nypelö, T., Salas, C., Arboleda, J., Hoeger, I. C., & Rojas, O. J. (2013).  
456 Cellulose nanofibrils. *1, 3, 1(3)*, 195-211.
- 457
- 458 [31] Boetker, J., Water, J. J., Aho, J., Arnfast, L., Bohr, A., & Rantanen, J. (2016). Modifying  
459 release characteristics from 3D printed drug-eluting products. *European Journal of*  
460 *Pharmaceutical Sciences*, 90, 47-52.
- 461
- 462 [32] Wang, L., Xu, H., Cooper, W. J., & Song, W. (2012). Photochemical fate of beta-blockers  
463 in NOM enriched waters. *Science of the total environment*, 426, 289-295.
- 464
- 465 [33] Siepman, J., & Siepman, F. (2012). Modeling of diffusion controlled drug delivery.  
466 *Journal of Controlled Release*, 161(2), 351-362.

- 467
- 468 [34] Siepmann, J., & Peppas, N. A. (2011). Higuchi equation: derivation, applications, use and  
469 misuse. *International journal of pharmaceutics*, 418(1), 6-12.
- 470
- 471 [35] Farah, S., Doloff, J. C., Müller, P., Sadraei, A., Han, H. J., Olafson, K., ... & Griffin, M.  
472 (2019). Long-term implant fibrosis prevention in rodents and non-human primates using  
473 crystallized drug formulations. *Nature Materials*, 1.
- 474
- 475 [36] Sandler, N., Salmela, I., Fallarero, A., Rosling, A., Khajeheian, M., Kolakovic, R., ... &  
476 Vuorela, P. (2014). Towards fabrication of 3D printed medical devices to prevent biofilm  
477 formation. *International journal of pharmaceutics*, 459(1-2), 62-64.
- 478
- 479 [37] Water, J. J., Bohr, A., Boetker, J., Aho, J., Sandler, N., Nielsen, H. M., & Rantanen, J.  
480 (2015). Three-dimensional printing of drug-eluting implants: preparation of an antimicrobial  
481 polylactide feedstock material. *Journal of pharmaceutical sciences*, 104(3), 1099-1107.

**Declaration of interests**

The authors declare that they have no known competing financial interests or personal relationships that could have appeared to influence the work reported in this paper.

The authors declare the following financial interests/personal relationships which may be considered as potential competing interests:

Journal Pre-proof